

PHOBEA/ITCT 2002 airborne observations of transpacific transport of ozone, CO, volatile organic compounds, and aerosols to the northeast Pacific: Impacts of Asian anthropogenic and Siberian boreal fire emissions

I. T. Bertschi,¹ D. A. Jaffe,^{1,2} L. Jaeglé,² H. U. Price,^{2,3} and J. B. Dennison¹

Received 4 November 2003; revised 6 March 2004; accepted 7 April 2004; published 14 July 2004.

[1] During the spring of 2002, vertical profiles of O₃, CO, nonmethane volatile organic compounds (VOCs), and total aerosol scattering were collected over the northwestern coast of Washington State as part of the University of Washington's Photochemical Ozone Budget of the Eastern North Pacific Atmosphere (PHOBEA) research campaign. These observations coincided with NOAA's Intercontinental Transport and Chemical Transformation 2002 (NOAA-ITCT 2K2) project. Thirteen research flights were conducted from 29 March through 23 May and several well-defined polluted layers of varying thickness (~0.2 to >3 km) were observed at altitudes between 0 and 6 km. These layers were characterized by correlated enhancements of O₃, CO, VOCs, and particles. We observed rapid transpacific transport of polluted air masses on 15 April and 14, 17, and 23 May 2002, with ΔO_3 and ΔCO (where Δ refers to the enhancement over background) exceeding 30 and 60 ppbv, respectively, and total aerosol scattering of green light ($\sigma_{\text{sp}}(550\text{ nm})$) exceeding 65 Mm^{-1} . These episodes were efficient in transporting O₃ to the northeast (NE) Pacific troposphere, with $\Delta\text{O}_3/\Delta\text{CO}$ ratios in the pollution layers varying from 0.22 to 0.42 mol mol⁻¹. In contrast, the average $\Delta\sigma_{\text{sp}}(550\text{ nm})/\Delta\text{CO}$ ratio of the mid-May events (0.66 ± 0.21 (1σ)) was more than twice that of the 15 April event (0.32 ± 0.05). The correlation between O₃, CO, aerosols, and VOCs coupled with back-trajectory analyses, satellite data, and the GEOS-CHEM global chemical transport model indicate that the primary source of pollution observed on 15 April originated from a mixture of Asian anthropogenic and biomass-burning emissions. For the May events, our analyses indicate that the early onset of the 2002 Siberian fire season was a significant source of the pollution episodes observed in May. **INDEX TERMS:** 0305 Atmospheric Composition and Structure: Aerosols and particles (0345, 4801); 0365 Atmospheric Composition and Structure: Troposphere—composition and chemistry; 0368 Atmospheric Composition and Structure: Troposphere—constituent transport and chemistry; **KEYWORDS:** long-range transport, ozone, aerosols

Citation: Bertschi, I. T., D. A. Jaffe, L. Jaeglé, H. U. Price, and J. B. Dennison (2004), PHOBEA/ITCT 2002 airborne observations of transpacific transport of ozone, CO, volatile organic compounds, and aerosols to the northeast Pacific: Impacts of Asian anthropogenic and Siberian boreal fire emissions, *J. Geophys. Res.*, 109, D23S12, doi:10.1029/2003JD004328.

1. Introduction

[2] Transpacific transport of trace gases and particles from the Eurasian continent to the northeast (NE) Pacific has been well established throughout the past 2 decades. To the best of our knowledge, *Andreae et al.* [1988] first provided detailed airborne-based measurements of the

long-range transport (LRT) of Eurasian emissions to the remote NE Pacific troposphere during May 1985. Many subsequent ground-based and airborne-based measurement campaigns have confirmed that under certain circumstances, trace gases including ozone (O₃), carbon monoxide (CO), radon, nitrogen oxides (NO_x), volatile organic compounds (VOCs), and particles of Eurasian origin may be transported to the NE Pacific within 5 to 6 days [*Kritz et al.*, 1990; *Parrish et al.*, 1992; *Jaffe et al.*, 1999, 2001, 2003; *McKendry et al.*, 2001; *Kotchenruther et al.*, 2001a; *Price et al.*, 2003, 2004]. Additionally, several studies have used Global Chemical Transport Models (GCTM) to quantify the impacts of Eurasian emissions on the NE Pacific troposphere [*Bernsten et al.*, 1999; *Jacob et al.*, 1999; *Jaeglé et al.*, 2003]. For example, using the GEOS-CHEM model, *Jaeglé et al.* [2003] suggest that the transport of Eurasian

¹Department of Interdisciplinary Arts and Sciences, University of Washington-Bothell, Bothell, Washington, USA.

²Department of Atmospheric Sciences, University of Washington, Seattle, Washington, USA.

³Department of Chemistry, University of Washington, Seattle, Washington, USA.

anthropogenic and biomass-burning emissions accounted for, on average, 17% of O₃ and 48% of CO in the NE Pacific lower troposphere (0–6 km above mean sea level (asl)) during the spring of 2001.

[3] Many different emission sources contribute to the trace gases and aerosols transported from Eurasia including uplifted mineral dust, natural and human-caused biomass fires, and fossil fuel and biofuel (e.g., wood, charcoal, and agricultural waste) combustion. Meteorological conditions play a key role in the transport of Eurasian emissions to the NE Pacific, particularly throughout the winter and spring [Merrill *et al.*, 1985, 1989; Hoell *et al.*, 1997; Newell and Evans, 2000; Liu *et al.*, 2003] when strong midlatitude westerly winds transport airmasses of Eurasian origin over the northwestern Pacific Ocean. Subsequently, the cyclonic rotation of the Aleutian Low coupled with the anticyclonic rotation of the Pacific High directs the Eurasian continental outflow toward the NE Pacific Ocean and western North America.

[4] To improve our understanding of the impacts of the LRT of Eurasian emissions, the University of Washington's Photochemical Ozone Budget of the Eastern North Pacific Atmosphere (PHOBEA) science initiative, which began in the spring of 1997, uses ground-based and airborne-based observations of O₃, CO, VOCs, and aerosols to help determine the influence Eurasian emissions have on O₃ photochemistry and the chemical composition of the NE Pacific troposphere and marine boundary layer (MBL) [Jaffe *et al.*, 1999, 2001, 2003; Kotchenruther *et al.*, 2001a, 2001b; Price *et al.*, 2003, 2004]. Prior to this study, two PHOBEA airborne campaigns were conducted in the springs of 1999 [Kotchenruther *et al.*, 2001a, 2001b] and 2001 [Price *et al.*, 2003]. The spring 2002 research flights were conducted concurrently with PHOBEA ground-based observations made at the University of Washington's Cheeka Peak Observatory, ("CPO," located at 48.3°N, 124.6°W and 480 m (asl)) [Weiss-Penzias *et al.*, 2004] and with the National Oceanic and Atmospheric Administration's Intercontinental Transport and Chemical Transformation 2002 (ITCT 2K2) research project (D. D. Parrish *et al.*, Intercontinental Transport and Chemical Transformation 2002 (ITCT 2K2) and Pacific Exploration of Asian Continental Emission (PEACE) Experiments: An overview of the 2002 winter and spring intensives, submitted to *Journal of Geophysical Research*, 2004).

[5] The primary goals of the PHOBEA 1999 and 2001 airborne studies included (1) investigating the impacts of Eurasian emissions on the composition and photochemistry of the NE Pacific troposphere and (2) investigating the relationships between measured species and the information these relationships provide about the emission sources. The goals of the PHOBEA 2002 airborne campaign are to add to the observations of the previous studies with particular interest in the relationships between O₃, CO, particles, and VOCs in polluted airmasses transported to the NE Pacific. In the 1999 and 2001 airborne studies, CO observations were made using canister sampling. In comparison, the 2002 airborne study was the first time we deployed a continuous ultraviolet resonance-fluorescence (UV-RF) CO instrument to compliment our measurements of O₃ and aerosol scattering, which greatly improved our capabilities for understanding CO-O₃-aerosol relationships. Because the

PHOBEA 2002 airborne campaign extended further into the spring than the previous two campaigns, a new and important finding of this study is the influence of Siberian biomass-burning emissions on the NE Pacific atmosphere during the late spring.

2. Experiment

[6] From 29 March through 23 May 2002 we conducted 13 flights using a small research aircraft (Beechcraft Duchess 76) over the NE Pacific Ocean (47.8°–48.5°N and 123.9°–125.4°W). A typical flight departed from Paine Field in Everett, Washington and ascended to ~6 km (asl) en route to the sampling location located west of CPO (Figure 1). Upon reaching this area, vertical profiles were collected during a spiraling descent to ~0.5 km (asl) followed by a return flight leg for a cumulative flight time of ~3.5 hours. Two rear-facing 1/4-inch o.d. (3/16-inch i.d.) inlets were used for the collection of canister whole air samples and continuous measurements of ambient air, respectively. A suite of instruments were employed for continuous measurements of O₃, CO, total aerosol scattering of light (σ_{sp}), ambient pressure, temperature, relative humidity (RH), and flight position (altitude, latitude, and longitude). The canister samples collected during each flight were subsequently analyzed for CO and VOCs. With the exception of the continuous CO instrument, the PHOBEA airborne measurement platform has been described elsewhere [Price *et al.*, 2003; Snow *et al.*, 2003], and therefore only a brief description of the measurement techniques are provided below.

2.1. Continuous Measurements

[7] Our flight track was mapped using a hand-held Global Positioning System (GPS) (Trimble, Inc.), which logged the flight coordinates every 5 s. Ambient temperatures and relative humidity (T/RH) were collected using a T/RH probe (Vaisala, Inc., model HMP 45), which extended ~20 cm from the outer skin of the aircraft. To assure the quality of these measurements, the temperature and relative humidity vertical profiles were compared with balloon-sonde measurements taken over Quillayute, Washington, located ~50 km southeast of CPO (available from the University of Wyoming's Department of Meteorology website at <http://weather.uwyo.edu/upperair/sounding.html>). For each flight we found an excellent agreement between our temperature and RH measurements and the sonde data.

[8] Ozone measurements were made using a miniature ultraviolet (UV) absorption analyzer (2B Technologies, Inc.) [Bognar and Birks, 1996], which has a precision and accuracy of ± 4 ppbv for 10-s signal averaging. An external O₃-CO-aerosol sampling inlet, consisting of a 15 cm stainless steel elbow (6.35 mm i.d.) and ~1.5 m of Teflon tubing (6.35 mm i.d.), brought outside air to the O₃ analyzer at a flow rate of ~15–20 L min⁻¹. Laboratory tests before and after the PHOBEA 2002 campaign indicated that at this flow rate no measurable O₃ losses or passivation effects occurred on the stainless steel or Teflon walls of the sample-inlet system.

[9] An integrating nephelometer (TSI, Inc., Model 3563) measured total aerosol scattering coefficients of blue, green, and red light (σ_{sp} (450 nm), σ_{sp} (550 nm), and σ_{sp} (700 nm)),



Figure 1. Map of the Pacific coastal region where vertical profiles were collected. Also shown are locations of major urban areas and the University of Washington's Cheeka Peak Observatory (CPO).

respectively. Owing to flow rates and the design of the rear-facing inlet, particles with a geometric diameter $>0.8 \pm 0.2 \mu\text{m}$ were excluded from these measurements [Price *et al.*, 2003; Jaffe *et al.*, 2003]. The nephelometer was calibrated with gases of known scattering coefficients (filtered air and CO_2) and has a total uncertainty of $\pm 0.2 \text{ Mm}^{-1}$ ($1 \text{ Mm}^{-1} = 1 \times 10^6 \text{ m}^{-1}$) or 11%, whichever is greater, for a 60-s averaging time. Zero-offsets of the instrument were determined during individual flights by flowing HEPA filtered air through the instrument en route to the vertical profiling location. Afterward, the scattering coefficients were corrected to standard temperature and pressure (STP (1 atm, 273 K)) and are reported as such throughout the remainder of this paper.

[10] In previous PHOBEA airborne campaigns, CO was measured exclusively using canister whole-air sampling with subsequent gas chromatography-reduction gas analyzer (GC-RGA) analysis. Up to eight canisters were sampled per flight, and thus the collection of highly resolved CO vertical profiles in the 0–6 km column was impractical. During the 2002 campaign, we continued to use canisters for CO analysis but also deployed an ultraviolet resonance-fluorescence (UV-RF) CO analyzer (Aerolaser, Inc., Model 5002) for collecting 1-s measurements of CO [Gerbig *et al.*, 1996, 1999]. In addition to the fast time response, the UV-RF CO instrument has high sensitivity (<2 ppbv for 10-s averaging time) and a detection limit of ~ 1.8 ppbv. Approximately three in-flight calibrations were performed per flight using a commercial CO standard in synthetic air (Scott Gas, Inc.), which was referenced to a primary laboratory CO standard (National Institute of Standards and Technology standard reference material, NIST-SRM) 2612a). The total estimated uncertainty of the UV-RF CO measurements is $\sim 5\%$ for a 10-s averaging time. Owing to logistical difficulties, the UV-RF CO analyzer was not operated during 4 of the 13 flights (Flights 1, 2, 4, and 6).

2.2. Canister Measurements

[11] A total of 81 whole-air canister samples were collected during the 2002 airborne campaign. Six canister samples were collected during each flight at altitudes of 6,

5, 4, 3, 2, and 0.5 km (asl) and two additional canisters were available during flights for sampling “layers of interest,” which were identified during our spiraling descent using the real-time O_3 , CO, and aerosol measurements. All whole-air samples were collected while maintaining a constant altitude (± 50 m) for ~ 2 –5 min. Subsequent to the research flights, the samples were analyzed for CO (as described above) and nonmethane VOCs using a cryogenic preconcentration injection technique with high-resolution gas chromatography separation and flame ionization detection (GC-FID). For a more detailed description of the techniques, we refer the reader to Doskey and Bialk [2001] and Price *et al.* [2003, 2004]. The precision of our RGA CO analysis, as determined from replicate measurements throughout the campaign, is $\sim 2\%$ with a total estimated uncertainty of $<5\%$.

2.3. Trajectory Analysis

[12] Back trajectories were calculated to determine the source regions for air masses in the vertical profiles using the NOAA Air Resources Laboratory (NOAA-ARL) Hysplit model (available at <http://www.arl.noaa.gov/ready/hysplit4.html>). The Hysplit model was operated with the National Center for Environmental Prediction's (NCEP) FNL meteorological data set and vertical motions were calculated using model vertical velocities. For each flight, the Hysplit model was used to calculate 10-day back trajectories at 500-meter intervals within the 0–6 km column at the sampling location and during the hour closest to the measurements.

2.4. Global Chemistry and Transport Model Analysis

[13] For atmospheric chemistry transport simulations and postmission analysis, we used the GEOS-CHEM global tropospheric chemistry model, version 5.03 (available at <http://www-as.harvard.edu/chemistry/trop/geos/>), which is driven by assimilated meteorology from the Goddard Earth Observing System (GEOS) of the NASA Global Modeling and Assimilation Office. The model simulates tropospheric O_3 - NO_x -VOC chemistry and includes ~ 120 chemical species and 24 tracers [Bey *et al.*, 2001a]. For the PHOBEA 2002 period, we used the GEOS-3 monthly meteorological fields at a horizontal resolution of 2° latitude by 2.5° longitude and at 30 vertical levels. The model's chemical mechanism, treatment of aerosols, emissions, transport, and deposition are described by Bey *et al.* [2001a] with recent updates by Martin *et al.* [2003]. The GEOS-CHEM model has been extensively evaluated against observations in many studies [Bey *et al.*, 2001a, 2001b; Li *et al.*, 2002a, 2002b; Palmer *et al.*, 2001, 2003; Fiore *et al.*, 2002; Jacob *et al.*, 2003; Liu *et al.*, 2002; Martin *et al.*, 2002]. These include recent comparisons to the PHOBEA 2001 airborne and ground-based observations [Jaeglé *et al.*, 2003], the PHOBEA 2002 ground-based observations [Liang *et al.*, 2004], and the ITCT-2K2 airborne observations (R. Hudman *et al.*, Ozone production in transpacific Asian pollution plumes and implications for ozone air quality in California, submitted to *Journal of Geophysical Research*, 2004).

[14] In addition to simulations with climatological biomass-burning emissions [Duncan *et al.*, 2003], we also conducted a simulation with enhanced CO emissions over

Siberia reflecting the early spring 2002 boreal fire season. In this simulation, CO was tagged according to source regions and emission type (e.g., Asian fossil fuel and biofuel, Southeast Asian biomass burning, and boreal biomass-burning emissions) and uses OH fields from the full chemistry simulation following *Bey et al.* [2001b] and *Jaeglé et al.* [2003]. We estimate that the April and May 2002 Russian boreal fires consumed a land area of ~ 4 million hectares [*Sukhinin et al.*, 2003; E. Hyer, personal communication, 2003]. Assuming 30 Mg of biomass were consumed per hectare [*Stocks*, 1991; *Cahoon et al.*, 1994, 1996; *Levine and Cofer*, 2000] and an emission factor of 120 g CO emitted per kg of biomass consumed [*Hegg et al.*, 1990; *Radke et al.*, 1991; *Susott et al.*, 1991; *Cofer et al.*, 1996; *Yokelson et al.*, 1997; *Goode et al.*, 2000], we estimate 14 Tg CO emitted from these fires during this period (4 Tg in April and 10 Tg in May). This is a factor of 4 higher than our climatological biomass-burning emission inventory. For comparison, global biomass-burning emissions for these 2 months account for, on average, 59 Tg CO, mostly due to biomass fires in Southeast Asia [*Duncan et al.*, 2003]. It has been noted elsewhere that the majority of fires in the Russian Far East appear to be crown fires [*Kasischke et al.*, 1999; *Kasischke and Bruhwiler*, 2002], although there is some debate on this issue [*Conard et al.*, 2002]. Because the high energy associated with boreal crown fires can lift smoke plumes into the free troposphere [*Cofer et al.*, 1996; *Lavoue et al.*, 2000], our “tagged-CO” simulation vertically distributes the Siberian biomass-burning emissions between 1.5 and 4.5 km above the surface.

3. Results and Discussion

3.1. Intercomparison of UV-RF and GC-RGA CO Measurements

[15] A comparison between the GC-RGA and UV-RF CO measurements is useful for validating the accuracy of the new UV-RF CO instrument. Figure 2 shows the GC-RGA CO measurements from the whole-air samples plotted against the continuous UV-RF CO. The UV-RF CO data in Figure 2 are the averages of the 1-s measurements collected during the corresponding period when a canister sample was collected (~ 4 min) and the error bars represent the variability (1σ) of the 1-s measurements within this time span. Typically, the variance in the UV-RF CO measurements was <5 ppbv, although in some of the highly polluted layers CO concentrations varied as much as 25 ppbv. Accounting for the combined uncertainties of the two measurement techniques, the near-unity slope (0.984 with y-intercept forced to zero) and the high R^2 value (0.951) indicate good agreement between the two instrumental methods and that no measurement biases were evident in either technique.

3.2. Intercomparison With the NOAA WP-3D Aircraft Measurements

[16] During Flight 10 (11 May), we conducted an intercomparison flight with the NOAA WP-3D research aircraft. The WP-3D and Duchess collected vertical profiles from ~ 2050 to 2115 and ~ 2135 to 2250 (UTC), respectively, within the 0–6 km column and over the region bounded by

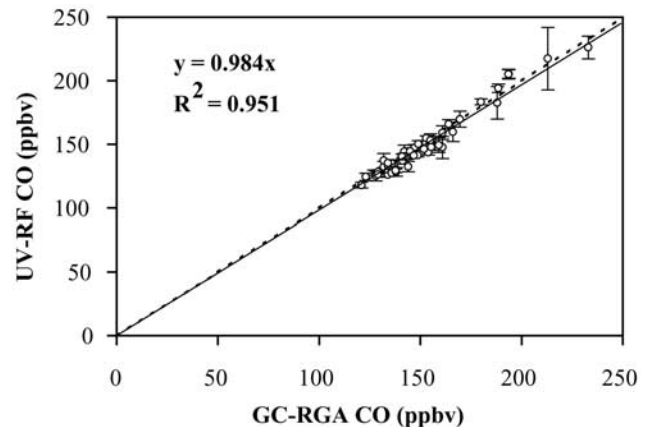


Figure 2. Plot of UV-RF versus GC-RGA CO measurements during this study. The UV-RF data have been averaged to the canister fill-time (~ 4 min) and the error bars represent the variability within a set of 1-s measurements. The solid line and the dashed line represent a least squares linear regression with the origin forced to zero and the one-to-one correlation line, respectively.

47.8° – 48.2° N latitude and 124.8° – 125.2° W longitude. Figure 3 shows a comparison of the O_3 and CO vertical profiles collected by both aircraft. Both aircraft observed similar major features in the CO vertical profiles with maximum concentrations of ~ 190 ppbv in a layer at 4.2 km. However, many of the minor features differ between the two profiles. The Duchess UV-RF CO values are usually higher (by as much as 8 ppbv) than those of the WP-3D. Similarly, in our comparison between the WP-3D and Duchess canister CO vertical profiles, the Duchess canister CO is also higher. We note that the differences are within the combined uncertainties of the measurements. Also, it is worth emphasizing that this was not a “wingtip-to-wingtip” intercomparison. Hence reasons for the differences between the collected CO vertical profiles may include real changes that occurred in the CO profile between the aircraft sampling times and slight discrepancies between primary CO standards employed by the research groups.

[17] There is good agreement between the two O_3 vertical profiles, as the average of the differences between the corresponding O_3 measurements throughout the 0–6 km column is less than 1 ppbv. However, Figure 3 shows that the Duchess O_3 profile is noisier than the WP-3D O_3 measurements and that the peaks of the two enhanced layers at ~ 4.2 and 5.5 km are not as well resolved in the Duchess O_3 profile as those in the WP-3D profile. This is likely due to the better precision and accuracy of the WP-3D O_3 instrument (1σ precision of 0.2 ppbv and 2% accuracy) compared with the UV absorption O_3 instrument used in this study (see section 2.1). Nonetheless, there is no evidence of bias between the two sets of O_3 observations.

3.3. Overview of the PHOBEA 2002 Airborne Measurements

[18] Table 1 provides a statistical summary of our measurements and Figure 4 shows the mean and median vertical profiles of O_3 , CO, σ_{sp} (550 nm), ethane (C_2H_6), methyl chloride (CH_3Cl), ethyne (or “acetylene,” C_2H_2), and

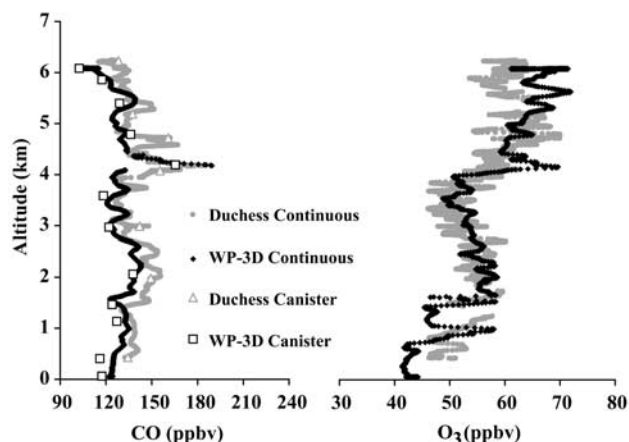


Figure 3. Vertical profiles of CO and O₃ collected by the NOAA WP-3D and UW Duchess research aircraft during Flight 10 (11 May 2002). Solid symbols denote continuous measurements and open symbols represent canister CO measurements.

propane (C₃H₈). Although we measured a total of nine VOCs, the four VOCs listed above accounted for ~90% of the total VOC (TVOC) mixing ratios quantified during PHOBEA 2002. We identified one canister sample (Flight 3, 1 km) that was likely contaminated by ship emissions and exclude this and other samples of regional pollution sources (Flights 5 and 6 at 1 and 2 km) from the data in Table 1 and Figure 4. The vertical profiles in Figure 4 illustrate the pronounced effects that the LRT of Eurasian

emissions had above the MBL. Specifically, O₃, CO, σ_{sp} (550 nm), and many VOCs peak between 3.5 and 5.5 km. Ethane, which comprised more than half of the TVOC observed in this study, generally decreases with increasing altitude with a minimum median value of 924 pptv at 6 km and a peak value of 1251 pptv in the 1-km bin. Similarly, C₂H₂ and C₃H₈ display the same general trend with peak median mixing ratios of 201 and 159 pptv, respectively, at 4 km. In contrast, CH₃Cl showed little variability throughout the 0–6 km column, with a mean of 582 ± 11 (1 σ) pptv.

3.3.1. Comparison of Airborne Observations With the GEOS-CHEM Model

[19] Figure 5 shows a comparison of the mean O₃ and CO vertical profiles from both the PHOBEA 2001 and 2002 observations and includes ensemble mean O₃ and CO vertical profiles from the GEOS-CHEM simulations, which uses data corresponding to the integrated flight times of the respective campaigns. Both simulations use the same climatological biomass-burning emission inventories. For comparison, Figure 5b also includes the mean O₃ and CO vertical profiles from the model simulations with the April and May 2002 Siberian biomass-burning enhancements (section 2.4). The model reproduces the 2001 CO observations reasonably well [Jaeglé *et al.*, 2003] but for O₃ the model displays a negative bias of 8 ppbv at the surface and, on average, a positive bias of ~5 ppbv above the MBL (Figure 5a). Figure 5b shows good agreement between the GEOS-CHEM model and the 2002 O₃ observations at 0–3 km and at 6 km, with a negative bias of ~0–3 ppbv at these altitudes for the simulation with the Siberian biomass-burning enhancements. However, the model displays a negative bias of ~7–10 ppbv at 4 and 5 km. Likewise,

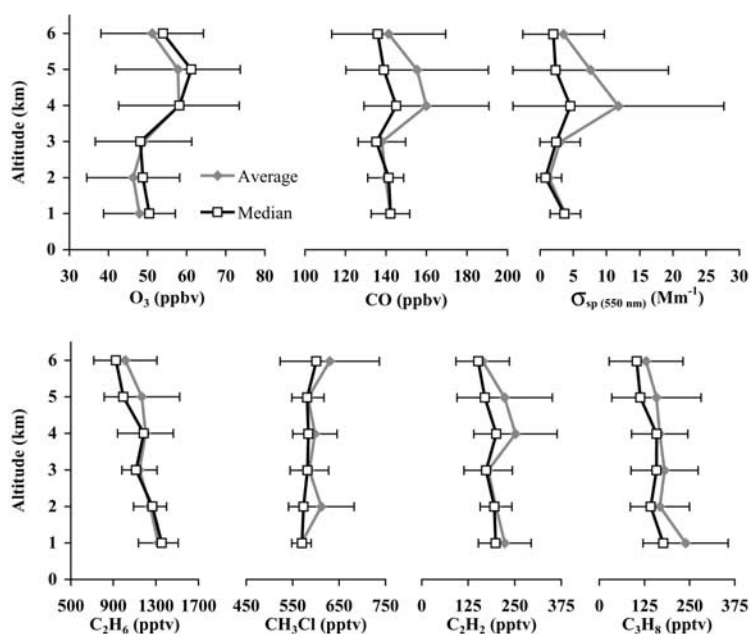


Figure 4. Vertical profiles of O₃, CO, VOCs, and aerosol scattering ($\lambda = 550$ nm) during the ITCT-PHOBEA 2002 airborne campaign. The means (closed diamonds), standard deviations of the means (1 σ , error bars), and medians (open squares) are derived from the 13 research flights after local (North American) pollution sources were removed.

Table 1. Trace Gases and Total Aerosol Scattering of Green Light ($\lambda = 550$ nm, σ_{sp} (550 nm)) From the Long-Range Transport of Eurasian and Pacific Airmasses Observed During the PHOBEA 2002 Campaign and Segregated by Altitude^a

Altitude Bin, km	O ₃ , ppbv	UV CO, ppbv	RGa CO, ppbv	$\sigma_{sp, 550nm}$, ^c Mm ⁻¹	Ethane, pptv	Methyl Chloride, pptv	Propane, pptv	Acetylene, pptv	Iso-butane, pptv	N-butane, pptv	N-pentane, pptv	N-hexane, pptv	Toluene, pptv	TVOC, ^d pptv
0.5–1.5	48 (9)	142 (10)	147 (10)	3.81 (2.30)	1278 (179)	568 (23)	229 (114)	205 (65)	22 (14)	37 (24)	6 (4)	2 (1)	12 (7)	2360 (338)
1.5–2.5	46 (12)	140 (9)	144 (8)	1.36 (1.88)	1244 (155)	612 (71)	168 (82)	200 (43)	22 (14)	39 (29)	18 (22)	4 (4)	14 (8)	2318 (299)
2.5–3.5	49 (12)	138 (12)	141 (12)	3.00 (3.04)	1145 (165)	586 (41)	180 (93)	178 (65)	19 (13)	27 (20)	22 (31)	3 (3)	11 (8)	2172 (340)
3.5–4.5	58 (15)	160 (31)	160 (25)	11.80 (15.88)	1202 (262)	598 (48)	167 (78)	252 (112)	19 (14)	31 (22)	14 (17)	3 (3)	13 (10)	2299 (476)
4.5–5.5	58 (16)	155 (35)	150 (33)	7.62 (11.71)	1168 (355)	583 (35)	158 (124)	223 (128)	19 (17)	30 (27)	21 (33)	4 (3)	12 (8)	2216 (638)
5.5–6.0	51 (13)	141 (28)	139 (20)	3.54 (6.12)	1013 (297)	630 (107)	130 (102)	164 (72)	16 (14)	28 (23)	18 (21)	4 (3)	11 (6)	2014 (543)
<i>Median</i>														
0.5–1.5	50	142	149	3.66	1251	570	177	191	14	21	5	2	11	2241
1.5–2.5	49	141	147	0.80	1267	574	142	195	19	30	10	2	13	2299
2.5–3.5	48	135	138	2.42	1113	582	158	173	14	20	10	2	9	2021
4.5–5.5	61	139	136	2.34	993	581	114	170	12	18	11	2	10	1922
5.5–6.0	54	136	132	1.99	924	601	104	152	12	22	15	3	11	1920
<i>Maximum and Minimum</i>														
0.5–1.5	75 27	167 110	158 127	12 bdl ^e	1507 1029	611 534	382 101	311 131	43 7	80 12	15 2	4 1	25 2	2903 1877
1.5–2.5	74 19	177 114	154 124	11 bdl ^e	1529 1028	758 546	290 52	269 122	56 7	110 8	78 bdl ^e	17 bdl ^e	27 4	2750 1788
2.5–3.5	79 18	207 111	166 122	39 bdl ^e	1505 824	702 546	423 80	338 49	47 7	82 9	90 1	9 1	32 4	3091 1775
3.4–4.5	100 18	277 115	213 129	68 bdl ^e	1595 686	719 557	320 20	481 137	61 5	97 5	64 3	14 bdl ^e	45 5	3366 1581
4.5–5.5	87 20	280 110	233 120	47 bdl ^e	1829 703	636 489	523 60	532 112	67 4	113 8	127 3	12 bdl ^e	31 4	3817 1540
5.5–6.0	79 18	292 107	189 120	48 bdl ^e	1629 664	962 538	358 30	358 82	51 1	91 2	83 2	13 1	30 5	3412 1374

^aFlight segments influenced by North American continental sources (Flights 5 and 6, <2.5 km) are not included.

^bStandard deviation (1σ) shown in parenthesis.

^cTotal aerosol scattering of green light (550 nm).

^dSum of the total quantified volatile organic compounds in this study.

^eBelow lower limit of detection.

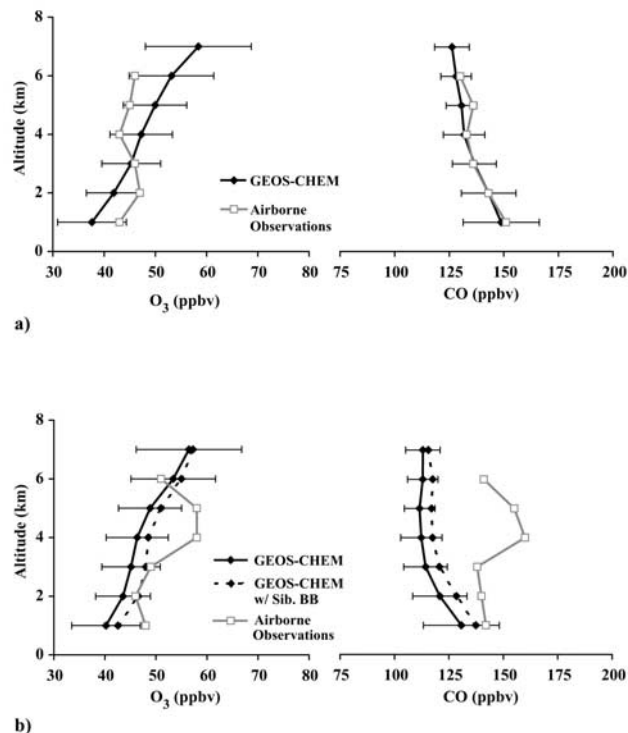


Figure 5. Comparison of the O_3 and CO vertical profiles produced from the GEOS-CHEM and airborne observations from (a) PHOBEA 2001 and (b) PHOBEA 2002. Both simulations use the same climatological biomass-burning emission inventories. The PHOBEA 2002 observations are compared with the GEOS-CHEM modeled vertical profiles with and without Siberian biomass-burning emission enhancements (see text).

the agreement between the 2002 CO observations and the model CO is reasonably good from the surface to 1 km, yet the model displays a negative bias of, on average, ~ 26 ppbv between 3 and 6 km. As noted in the previous section, these were the altitudes where the observed enhancements of trace gases and particles due to LRT are most pronounced. This suggests an additional source (or sources) of ozone, CO, aerosols, and VOCs during the 2002 study in comparison with the 2001 study.

[20] Figure 6 shows the GEOS-CHEM time-height cross sections from the simulation of three tagged CO tracers transported to CPO (48.3°N , 124.6°W) from Asian CO (including fossil fuel and biofuel emissions) (Figure 6a), Asian biomass-burning CO from southeast (SE) Asia (Figure 6b), and Asian biomass-burning CO emissions from boreal fires in Russia (Figure 6c) with enhanced emissions reflecting the early spring 2002 boreal fire season. Figure 6 also includes the times when the 2002 airborne observations were made between 25 March and 27 May 2002 (indicated by black vertical lines and flight number). From mid to late April, Asian anthropogenic sources account for ~ 30 – 60 ppbv of the tagged-CO near the surface. Enhanced CO levels were also observed at CPO during these long-range transport events [Weiss-Penzias *et al.*, 2004; Liang *et al.*, 2004]. In contrast, most of the SE Asian biomass-burning CO contribution (~ 15 – 30 ppbv) was above ~ 3 – 4 km. In comparison with the former two sources, the GEOS-CHEM simulation estimates that Siberian biomass-burning CO increases in

frequency and magnitude throughout the lower troposphere from mid-April through May 2002.

3.3.2. Case Studies of 2002 Long-Range Transport Events

[21] Here we present four case studies of LRT observed during PHOBEA 2002. The term “event” describes episodes of transpacific transport based on the following criteria: (1) CO and $\sigma_{sp(550\text{ nm})}$ must be elevated relative to monthly median levels by >50 ppbv and 20 Mm^{-1} , respectively; (2) local winds must be consistently from the Pacific and away from any regional pollution sources for the duration of the event; (3) trajectories must be consistent with the local winds and indicate transpacific transport.

3.3.2.1. Flight 3 (15 April 2002)

[22] Figure 7 shows the vertical profiles of Flight 3, which was the first LRT event observed during PHOBEA 2002. From 10 to 15 April 2002, the Pacific High was at ~ 45 – 55°N latitude and 165 – 175°W longitude and the Aleutian Low was located over the northeastern Gulf of Alaska (~ 50 – 60°N , 130 – 150°W). This system conducted westerly winds from the Northwest Pacific to the Washington state coastline. Meteorological conditions were characterized by westerly winds throughout the 0–6 km column and a low cloud layer extending from 0.5 to 3 km. A layer of enhanced pollutants was present from 3 to 6 km. Ozone, CO, and $\sigma_{sp(550\text{ nm})}$ levels in the polluted layer exceeded 85 ppbv, 270 ppbv, and 50 Mm^{-1} , respectively. In addition, most of the VOCs observed between 3 and 6 km were significantly enhanced and accounted for

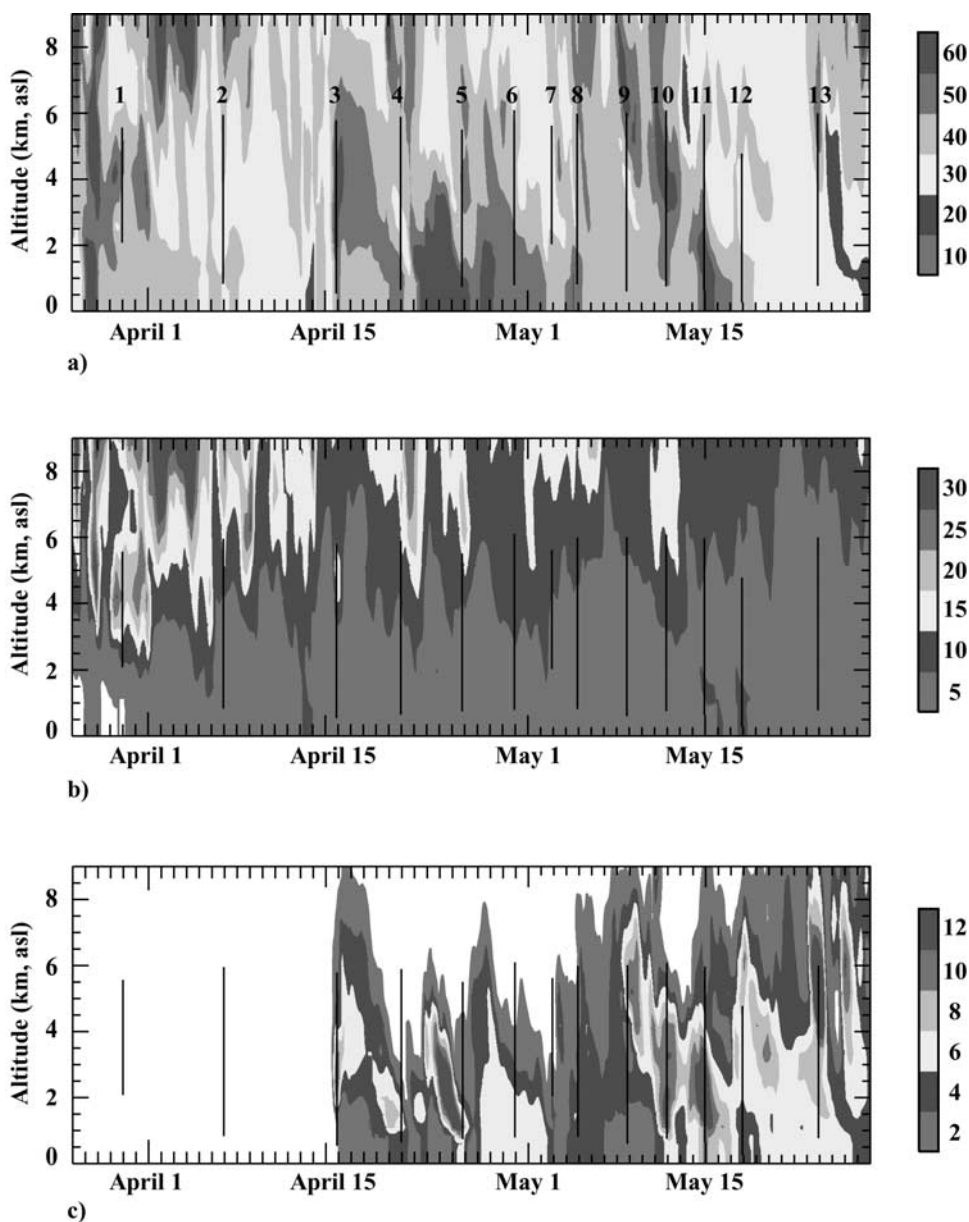


Figure 6. GEOS-CHEM time-height cross sections of the tagged-CO simulation at CPO (48.3°N, 124.6°W) throughout the spring of 2002. The numbered vertical lines show the vertical range of the PHOBEA 2002 research flights. The cross sections show (a) Asian anthropogenic, (b) Southeast Asian biomass burning, and (c) Siberian biomass burning sources of CO. Note that each CO cross section is scaled differently. See color version of this figure at back of this issue.

the maximum VOC mixing ratios observed during this study.

[23] In previous years, springtime LRT events in the NE Pacific have contained a significant component of desert dust [Jaffe *et al.*, 1999, 2001, 2003; Husar *et al.*, 2001; Price *et al.*, 2003, 2004]. Therefore we used our aerosol scattering data to investigate the possibility that mineral dust may have been entrained in this polluted airmass. Price *et al.* [2003] have shown that the Ångström exponent, \mathring{a} , calculated from our nephelometer data is a good indicator of mineral dust. The Ångström exponent is calculated using equation (1):

$$\mathring{a}(\lambda_1/\lambda_2) \equiv -\log(\sigma_{sp(\lambda,1)}/\sigma_{sp(\lambda,2)})/\log(\lambda_1/\lambda_2). \quad (1)$$

In general, scattering measurements of mineral dust and coarse mode particles provide lower Ångström exponents (~ 1 to 1.5) than fine mode particles (~ 2 to 2.5). The $\mathring{a}(\lambda_{550}/\lambda_{700})$ in the 3–6 km column was, on average, 2.1 ± 0.3 (1σ), indicating a lack of dominance of coarse mode particles in the aerosol mode distribution of this event.

[24] This event was also captured by the GEOS-CHEM model, which assigns its origins to Asian anthropogenic emissions (30–40 ppbv CO) with smaller contributions from biomass burning (<20 ppbv CO). Figure 8 shows the 10-day Hysplit back trajectories and the time-height profiles of this event. Figure 8 also includes NASA/MODIS active fire detections made from 5 to 11 April 2002 (made available through the University of Maryland at <http://>



Figure 7. Vertical profiles of O₃, CO, VOCs, and aerosol scattering ($\lambda = 550 \text{ nm}$) during the 15 April event. The VOC measurements in the marine boundary layer (<1 km) showed evidence of local ship exhaust (see text) and not included.

firemaps.geog.umd.edu). For a detailed discussion of the MODIS fire products, we refer the reader to *Justice et al.* [2002]. The MODIS fire detections have a resolution of $1^\circ \times 1^\circ$ and indicate that the highest fire activity at this time was in Southeast Asia ($\sim 30\text{--}15^\circ\text{N}$, $90\text{--}120^\circ\text{E}$). The back trajectories for this event indicate that most of the air masses we observed during the 15 April event passed through the region within $35\text{--}45^\circ\text{N}$ latitude and $110\text{--}140^\circ\text{E}$ longitude and were uplifted from $\sim 2\text{--}4 \text{ km}$ (above ground level, agl) to $4\text{--}8 \text{ km}$ (agl), followed by rapid transport ($\sim 4\text{--}5 \text{ days}$) across the Pacific Ocean.

3.3.2.2. Flights 11–13 (14, 17, and 23 May 2002)

[25] Figures 9a–9c illustrate the vertical profiles of the major trace gases and total aerosol scattering ($\sigma_{sp}(550 \text{ nm})$) for Flights 11–13 (14, 17, and 23 May, respectively), which we refer to collectively as the “May events.” The largest of these events was observed during Flight 12 (Figure 9b). A dry, polluted layer was observed above 3.5 km atop a moist and much less polluted airmass that extended down to the MBL. Within the polluted layer, O₃, CO, C₂H₆, C₂H₂, C₃H₈, and $\sigma_{sp}(550 \text{ nm})$ were all enhanced relative to their May 2002 median levels by $\sim 25 \text{ ppbv}$, 80 ppbv , 350 pptv , 100 pptv , 250 pptv , and 40 Mm^{-1} , respectively, with only a slight enhancement in CH₃Cl (<10 pptv). A sharp concentration gradient in O₃, CO, and $\sigma_{sp}(550 \text{ nm})$ was observed at $\sim 3.5 \text{ km}$, where the levels of these species plummeted by $\sim 40 \text{ ppbv}$, 80 ppbv , and 40 Mm^{-1} , respectively.

[26] Figures 9a and 9c show the respective vertical profiles observed during Flights 11 and 13. While the layers of interest were vertically narrower than the 17 May event, these layers show similar enhancements of O₃ ($10\text{--}20 \text{ ppbv}$), CO ($40\text{--}70 \text{ ppbv}$), and $\sigma_{sp}(550 \text{ nm})$ ($30\text{--}60 \text{ Mm}^{-1}$). In addition, Flight 13 had the largest $\sigma_{sp}(550 \text{ nm})$ and O₃ mixing ratios observed during this study (68 Mm^{-1} and $\sim 100 \text{ ppbv}$, respectively). Similar to the 17 May event, almost all VOCs exhibited significant

enhancements that were correlated with the enhancements of O₃, CO, and $\sigma_{sp}(550 \text{ nm})$. Additionally, the Ångström exponent, $\hat{a}(\lambda_{550}/\lambda_{700})$, determined from the aerosol scattering data collected during these events varied from 2.3 to 2.4, indicating a submicron aerosol size distribution.

[27] Figures 10a–10c show the NOAA Hysplit trajectories for the May events superimposed over the maps of the NASA/MODIS active fire detections for 1–6 May (Figure 10a), 7–13 May (Figure 10c), and 14–19 May (Figure 10c) 2002. The backward trajectories indicate that the polluted airmasses observed during May originated from areas near the southeast Russian border with China and Mongolia, and the MODIS fire detections indicate that the highest fire activity in early May 2002 was between $\sim 45^\circ$ and 60°N latitude. We note that all of the May events originate from a vast area but that the high frequency of fire detections in these areas indicate that biomass-burning emissions are likely a significant contribution to the May events. We also note that the 14 May back trajectories (Figure 10a) started near a region in southeastern Russia ($\sim 40\text{--}50^\circ\text{N}$, $120\text{--}150^\circ\text{E}$) dominated by fire activity and subsequently passed over central Japan at $3\text{--}4 \text{ km}$ above ground level (agl) before transport across the Pacific. In contrast, the 14 and 23 May events were transported over the Pacific at much higher latitudes ($>50^\circ\text{N}$), yet originated from regions also dominated by fire activity. As indicated by the GEOS-CHEM model, emissions from several other sources (both anthropogenic and natural) mixed in with the LRT plumes. However, our observations, coupled with the satellite data, back-trajectories, and the GEOS-CHEM model (discussed below), indicate that the Siberian fires are a predominant source of the May events.

[28] As noted earlier, the GEOS-CHEM model predicts enhanced transport of CO from Siberian fires for all three May events profiled here, yet the magnitude is relatively small ($2\text{--}12 \text{ ppbv}$) compared with our airborne observa-

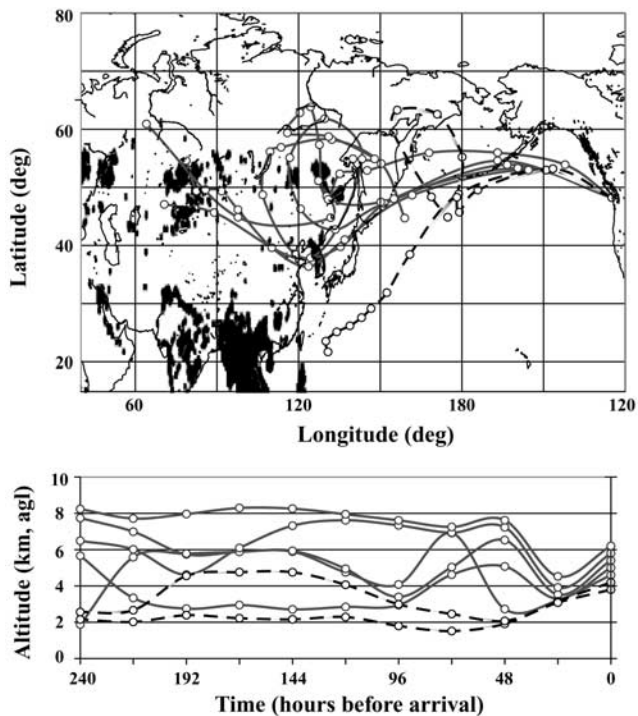


Figure 8. The NOAA Hysplit back trajectories for the upper air mass (~ 3.5 to 6 km) observed during 15 April 2002. Also shown are active fires detected in Asia from 5 to 11 April 2002 by the NASA TERRA/MODIS satellite. Each marker represents active fire detections within a $1^\circ \times 1^\circ$ grid. The bottom plot shows the temporal profiles of the altitudes (above ground level, agl) of the individual back trajectories.

tions (40–70 ppbv). These discrepancies are most likely due to uncertainties in CO emission factors, burned area estimates, coarse vertical resolution of the model (~ 1 km), and/or excessive dilution of emissions during transport in the model. It is worth noting that the model captures the altitude ranges (2–5 km) where the Siberian LRT events are observed. In a simulation where we limit emissions to the boundary layer, the modeled CO enhancements are generally weaker and restricted to altitudes below 2 km. The model simulations were not sensitive to the maximum height of emissions (which we varied between 2.5 and 4.5 km), as long as some emissions were injected above the boundary layer. This underscores the importance of the injection height on the global fate of biomass-burning emissions.

3.3.3. Enhancement Ratios of the 2002 Events

[29] Here we detail our observations of O_3 -CO-aerosol relationships to provide further insight into the LRT events. The observed correlations between CO, O_3 , particles, and VOC in the aged haze layers of the 2002 events are indicative of combustion sources. The difference between the CO concentrations in a polluted air mass from that of the CO concentrations in the background air ($\Delta CO = CO_{\text{pollution}} - CO_{\text{bkg}}$) can be used to normalize the excess mixing ratio of a coemitted species (i.e., $\Delta X/\Delta CO$). While O_3 is not a primary emission, significant levels of O_3 are produced downwind when CO, CH_4 , and VOCs react with hydroxyl radicals (OH) in the presence of NO_x and sunlight.

Because CO is indicative of combustion sources and has a relatively long lifetime in the troposphere, $\Delta O_3/\Delta CO$ (defined as the “enhancement ratio” or “ER”) is commonly used as an indicator of photochemical O_3 production in polluted air masses originating from combustion processes [Wofsy et al., 1992; Jacob et al., 1992; Parrish et al., 1993; Mauzerall et al., 1996, 1998; Goode et al., 2000; Forster et al., 2001; Yokelson et al., 2003; Hobbs et al., 2003; Price et al., 2004].

[30] The determination of the background concentration of CO and trace gases can be problematic. A common method employed in airborne studies is to collect background measurements at approximately the same height but outside of the polluted layer of interest [Goode et al., 2000; Yokelson et al., 2003; Hobbs et al., 2003]. In airborne measurements of LRT this is impractical, since haze layers are often dispersed horizontally over a large region. A more practical approach uses the measurements of unpolluted air masses above and below the polluted layer as a background. However, this too may be problematic when a polluted layer extends above the maximum sampling altitude (e.g., Flight 12) or when the boundary between the haze and background are poorly delineated. To overcome these difficulties, we employed two methods. First, we used the April and May median vertical profiles, respectively, to simulate the background concentrations during the events. Second, the monthly backgrounds were compared with the backgrounds determined by the clean layers above and below the polluted layer for each event. For Flights 3 and 12 only the air masses below the polluted layers were used as a background reference.

[31] Table 2 lists the enhancement ratios and excess mixing ratios for all species measured during the four PHOBEA 2002 events. The $\Delta O_3/\Delta CO$ and $\Delta \sigma_{\text{sp}}(550 \text{ nm})/\Delta CO$ values are reported with respect to the UV-RF CO observations, and the VOC ERs are given with respect to the corresponding canister RGA CO measurements. For each event, the continuous measurements of O_3 , CO, and $\sigma_{\text{sp}}(550 \text{ nm})$ were averaged every 100 m within the polluted air masses before calculating the ER. Measures were taken to avoid including O_3 , CO, and σ_{sp} values from the “clean” layers above and below the well-delineated boundaries of the pollution layers while calculating the 100-m averages. Subsequently, the 100-m average ΔO_3 , ΔCO , and $\Delta \sigma_{\text{sp}}(550 \text{ nm})$ values were used to determine $\Delta O_3/\Delta CO$ and $\Delta \sigma_{\text{sp}}(550 \text{ nm})/\Delta CO$ values for every 100-m interval. Finally, within each plume, the “100-m” ERs were segregated with respect to the altitudes where canisters were collected and averaged with respect to the time of the canister measurements.

3.3.3.1. Ozone Enhancement Ratios

[32] The observed $\Delta O_3/\Delta CO$ values during the 2002 events vary from 0.22 to 0.42 ppbv ppbv $^{-1}$ and are comparable to the range of $\Delta O_3/\Delta CO$ values reported in aged (>24 hours) emissions from previous field studies conducted at middle and high northern latitudes [Wofsy et al., 1992; Mauzerall et al., 1996; Wotawa and Trainer, 2000; Forster et al., 2001]. For example, during a 1990 summer field study conducted at high latitudes in North America, Mauzerall et al. [1996] report $\Delta O_3/\Delta CO$ ratios ranging from ~ 0.11 to 1.3 within aged anthropogenic pollution plumes and from ~ 0 to 0.66 in aged biomass-burning plumes. They attributed the lower $\Delta O_3/\Delta CO$ ratios

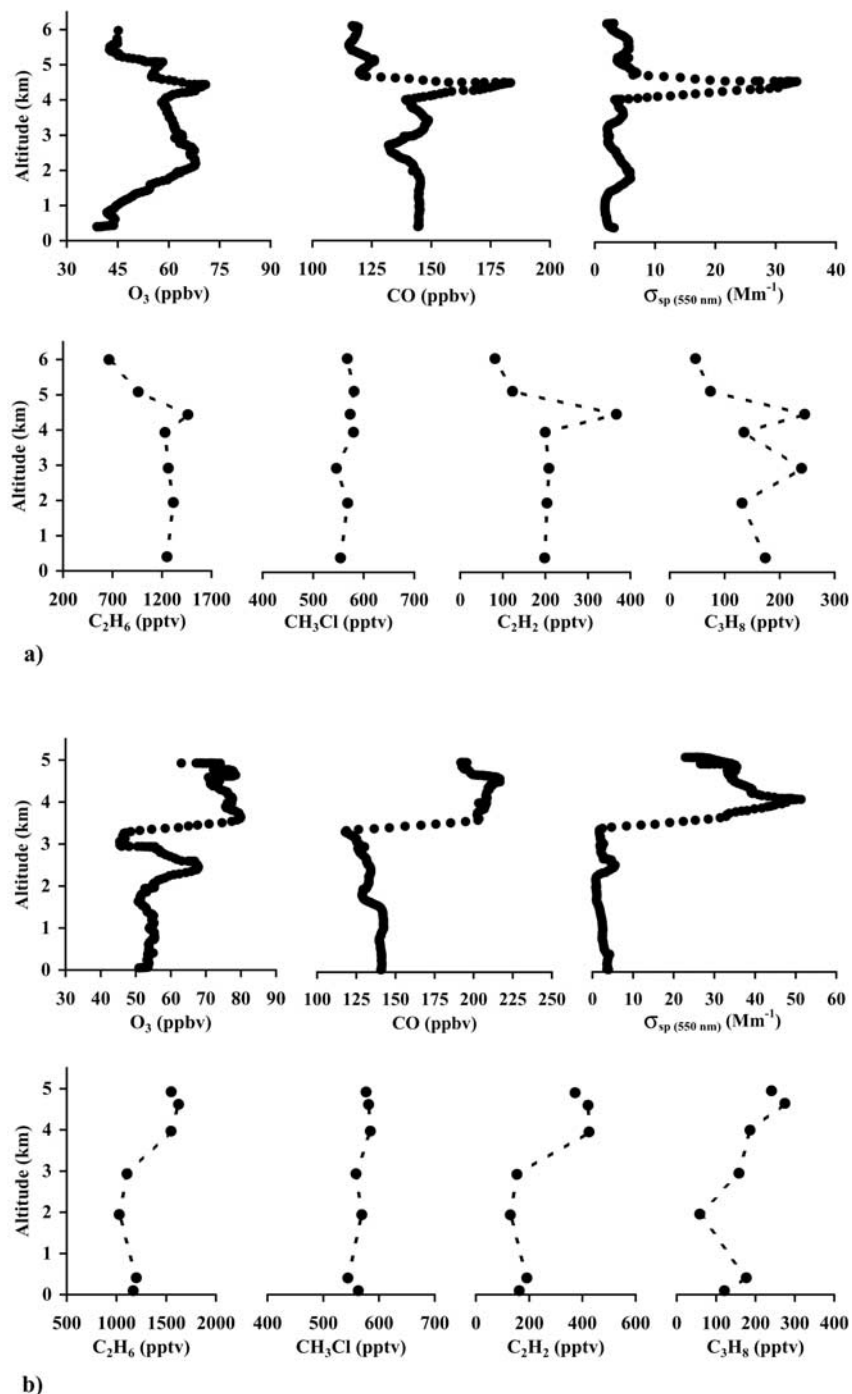


Figure 9. Same as Figure 7 but for the May events: (a) 14 May, (b) 17 May, and (c) 23 May 2002. Correlated enhancements of O_3 , CO, total aerosol scattering ($\lambda = 550$ nm), and most VOCs are evident above 3.0 km in all of the profiles.

observed in the biomass-burning plumes to lower NO_x emissions from biomass burning compared with that of urban and industrial combustion processes.

[33] In this study, the highest $\Delta O_3/\Delta CO$ ratio was measured within the 15 April plume, yet this plume also had the highest variability (0.26–0.42) as $\Delta O_3/\Delta CO$ ratios decreased with increasing altitude. This trend was also observed for the $\sigma_{sp(550\text{ nm})}$, C_2H_2 , and C_3H_8 ERs, while the C_2H_6 and C_4H_{10} ERs remained consistent throughout

the plume. Because of the variability in the enhancement ratios of the VOCs with similar or longer atmospheric lifetimes than CO (e.g., C_2H_2 and CH_3Cl), it appears likely that the 15 April event was not as well-mixed compared with the 17 May event. Again, the GEOS-CHEM model predicted an enhancement in Asian CO for 15 April with a dominant contribution from Asian anthropogenic sources during this event. The $\Delta O_3/\Delta CO$ ratios observed during all four events are in reasonably

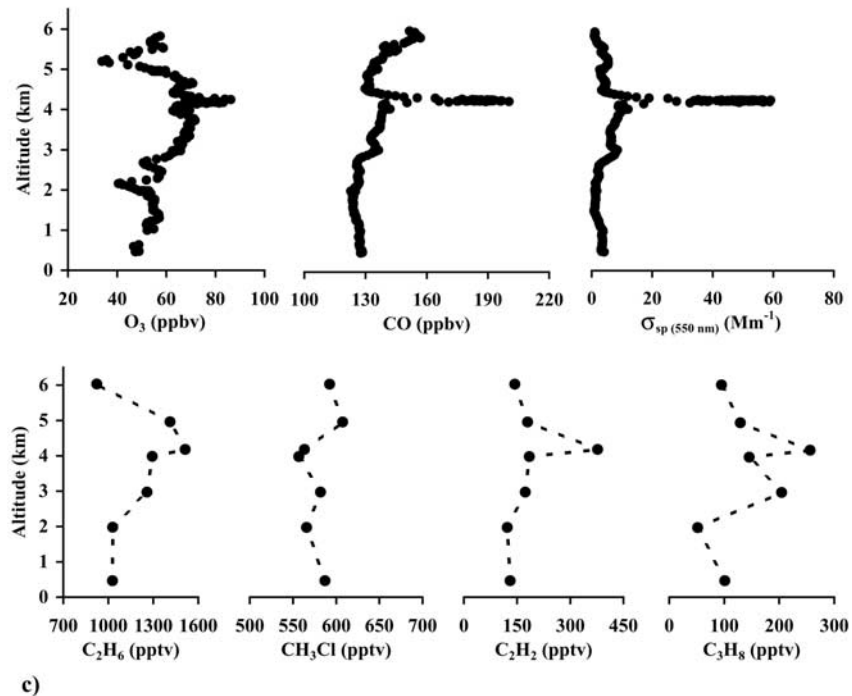


Figure 9. (continued)

good agreement with an “event” $\Delta\text{O}_3/\Delta\text{CO}$ mean value of 0.29 ± 0.07 (1σ). This is in contrast to highly variable O_3 enhancements relative to CO in previously observed LRT events in the NE Pacific (e.g., $\Delta\text{O}_3/\Delta\text{CO} = -0.06$ to $1.52 \text{ mol mol}^{-1}$) [Jaffe *et al.*, 2003; Price *et al.*, 2004],

which included surface events and at least one large mineral dust event.

3.3.3.2. Aerosol and VOC Enhancement Ratios

[34] In contrast to the ozone ERs, the $\Delta\sigma_{\text{sp}(550 \text{ nm})}/\Delta\text{CO}$ ratios for the 2002 events are highly variable. For example,

Table 2. Excess Mixing Ratios and Enhancement Ratios, ER (Relative to CO), of the Airborne Measurements Collected During the Four PHOBEA 2002 Events^a

Species	15 April			14 May		17 May		23 May
	6.5–5.5 km	5.5–4.5 km	4.5–3.5 km	4.5–4.2 km	6.5–5.5 km	5.5–4.5 km	4.5–3.5 km	4.4–4.1 km
<i>Excess Mixing Ratios</i>								
UV-Rf CO, ppbv	106	109	69	41	60	64	71	47
O_3 , ppbv	27	32	29	11	15	17	15	17
$\sigma_{\text{sp}(550 \text{ nm})}$, Mm^{-1}	29	35	24	31	30	34	36	46
GC-RGA CO, ppbv	62	108	68	36	54	59	50	44
Ethane, pptv	680	992	623	367	551	625	455	418
Ethyne, pptv	198	396	306	173	209	258	231	183
Propane, pptv	277	409	216	110	147	182	51	121
N-butane, pptv	69	100	78	11	28	21	8	10
Iso-butane, pptv	38	58	49	3	12	10	3	8
N-pentane, pptv	6	122	26	4	0	0	1	5
Toluene, pptv	0	12	33	5	0	1	0	2
Methyl chloride, pptv	352	0	120	0	0	0	5	0
N-hexane, pptv	1	11	9	0	1	1	0	0
<i>Enhancement Ratios (mol mol^{-1})</i>								
$\Delta\text{O}_3/\Delta\text{CO}$	0.26	0.30	0.42	0.28	0.24	0.27	0.22	0.36
$\Delta\sigma_{\text{sp}(550 \text{ nm})}/\Delta\text{CO}$	0.27	0.32	0.36	0.77	0.51	0.52	0.51	0.99
$\Delta\text{ethane}/\Delta\text{CO}$	0.0110	0.0092	0.0092	0.0102	0.0103	0.0106	0.0092	0.0094
$\Delta\text{ethyne}/\Delta\text{CO}$	0.0032	0.0037	0.0045	0.0048	0.0039	0.0044	0.0047	0.0041
$\Delta\text{propane}/\Delta\text{CO}$	0.0045	0.0038	0.0032	0.0031	0.0027	0.0031	0.0010	0.0027
$\Delta\text{n-butane}/\Delta\text{CO}$	0.0011	0.0009	0.0012	0.0003	0.0005	0.0004	0.0002	0.0002
$\Delta\text{i-butane}/\Delta\text{CO}$	0.0006	0.0005	0.0007	0.0001	0.0002	0.0002	0.0001	0.0002
$\Delta\text{n-pentane}/\Delta\text{CO}$	0.0001	0.011	0.0004	0.0001	-	-	-	0.0001
$\Delta\text{toluene}/\Delta\text{CO}$	-	0.0001	0.0005	0.0001	-	-	-	0.0000
$\Delta\text{methyl chloride}/\Delta\text{CO}$	0.0057	-	0.0018	-	-	-	0.0001	-
$\Delta\text{n-hexane}/\Delta\text{CO}$	-	0.0001	0.0001	-	-	-	-	-

^aOzone and $\sigma_{\text{sp}(550 \text{ nm})}$ ER are reported relative to the UV-RF CO and VOC ER are reported relative to RGA CO.

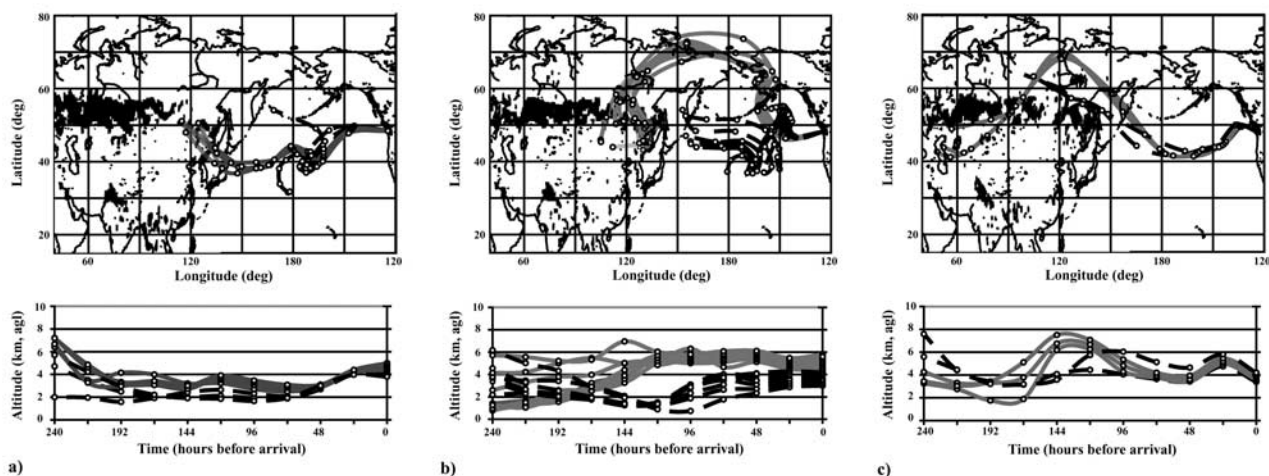


Figure 10. Same as Figure 8 but for the polluted layers measured during (a) 14 May, (b) 17 May, and (c) 23 May 2002. The NASA/MODIS fire detections in Figures 10a–10c show detections made from 1–6 May (Figure 10a), 7–13 May (Figure 10b), and 14–19 May (Figure 10c) 2002, respectively.

the average $\Delta\sigma_{\text{sp}}(550\text{ nm})/\Delta\text{CO}$ during the May events (0.66 ± 0.22) is more than twice that of the 15 April event (0.31 ± 0.04), possibly due to greater particle deposition or a relatively smaller aerosol source for the 15 April event. However, the HYSPLIT4 model indicates that the 15 April event had a shorter transit time than the May events, remained above the MBL during transit, and was subjected to little precipitation during transport. Thus the difference between the $\Delta\sigma_{\text{sp}}(550\text{ nm})/\Delta\text{CO}$ values is most likely due to relatively high particle emission rates (with respect to CO) at the source regions of the May events, which is typical of smoke from large, high-intensity biomass fires [Ward and Hardy, 1991; Radke et al., 1991; FIRESCAN Science Team, 1996; Reid and Hobbs, 1998; Reid et al., 1998].

[35] With the exception of methyl chloride, the VOCs in Table 2 have similar or shorter atmospheric lifetimes than that of CO. Assuming significant VOC losses during transport (relative to CO) from reaction with OH, the ERs presented in Table 2 may be considered lower limits to the emission ratios of these VOCs at the source regions. Butane, 2-methyl-propane, pentane, toluene, and hexane all have atmospheric lifetimes $\sim <4$ days and make up $<5\%$ of the total excess VOCs measured during each of the May events. Ethane, emitted from both biomass and fossil fuel combustion, has a similar lifetime to that of CO and has the highest ER ($\sim 9.9 \pm 0.7 \times 10^{-3} \text{ mol mol}^{-1}$) of all the VOCs.

[36] The CH_3Cl ERs vary significantly between the April and May events with a maximum $\Delta\text{CH}_3\text{Cl}/\Delta\text{CO}$ value of $5.7 \times 10^{-3} \text{ mol mol}^{-1}$ observed during the 15 April event and negligible enhancements observed during the May events. Methyl chloride has an atmospheric lifetime of approximately 0.5–1 year, which is much longer than that of CO, indicating that the variations between the April and May events are primarily due to different sources and/or emission rates and not atmospheric removal processes. The absence of enhanced CH_3Cl in the May events is particularly interesting because biomass burning is considered a major global source of CH_3Cl [Crutzen et al., 1979; Andreae et al., 1996; Blake et al., 1996; Lobert et al., 1999]. However, CH_3Cl emissions are known to vary

significantly by fuel and fire type. For example, in their overview of emissions from global biomass burning, Andreae and Merlet [2001] present a compilation of laboratory and field measurements that indicate CH_3Cl emission rates can vary by as much as an order of magnitude. Using the data presented by Andreae and Merlet [2001] (and references therein), the predicted CH_3Cl emission ratio relative to CO for extratropical fires is $\sim 3.0 \pm 2.0 \times 10^{-4} \text{ mol mol}^{-1}$. Using this estimate with the maximum ΔCO value observed on 17 May (71 ppbv), we predict a CH_3Cl enhancement of $21 \pm 14 \text{ pptv}$, which is only $\sim 4\%$ of ambient CH_3Cl concentrations observed during the 2002 spring. Therefore the lack of enhanced CH_3Cl in the May events does not necessarily exclude biomass burning as the primary source of the May events.

[37] Finally, it is important to note that agricultural residue burning is prevalent throughout regions of Asia and that a relatively high number of Asian households use biofuels (wood, charcoal, and dung cakes) as a primary energy source [Streets and Waldhoff, 1999]. During the recent TRACE-P study, observations made in Asian urban plumes indicated high levels of CH_3Cl and HCN, indicating that Asian urban areas are a significant source of emissions from the combustion of agricultural residue and wood biofuels [Jacob et al., 2003; Li et al., 2003; Blake et al., 2003]. Compared with temperate and boreal fires, biofuel and tropical fires may emit larger amounts of CH_3Cl relative to CO [Andreae and Merlet, 2001]. Therefore the correlation of enhancements of CH_3Cl with CO, aerosols, and hydrocarbons suggest that the observed pollutants in the 15 April event had a component from biofuel and/or tropical biomass fires. Furthermore, as noted in section 3.3.2.1, the GEOS-CHEM model predicts that a significant fraction of the observed pollutants in the 15 April event originated from Southeast Asian biomass burning.

4. Summary and Conclusions

[38] In this study we made airborne measurements of trace gases and aerosols in the northeast (NE) Pacific

troposphere during the ITCT-PHOBEA spring 2002 research campaign. This was the third PHOBEA airborne campaign but the first time we used a new UV-RF CO instrument for continuous measurements of CO to complement our continuous observations of O₃ and aerosols. A comparison of the UV-RF CO technique and our canister CO measurements showed that there was a good agreement between the methods with no evident measurement biases. Furthermore, this was the first campaign that we were able to conduct an intercomparison of our airborne observations with a separate airborne measurement platform. In our comparison with the NOAA WP-3D research aircraft, we found a generally good agreement between corresponding measurements; the most important of these were O₃ and CO. There was a good agreement between O₃ observations, although our O₃ vertical profile was slightly noisier due to electrical noises that have since been addressed. Our CO measurements displayed a slight difference relative to the NOAA WP-3D measurements by ~1–8 ppbv but agree within the combined uncertainties of the measurement techniques.

[39] An overview of the vertical profiles of trace gases and particles throughout the NE Pacific troposphere (0–6 km) during the 2002 spring indicates that LRT of Eurasian emissions had the most significant impacts above 2 km. Specific episodes of the LRT of polluted air masses were identified on 15 April and 14, 17, and 23 May 2002. Observations of aerosol scattering and VOC enhancement ratios (relative to CO) coupled with back trajectories, remote sensing of biomass fires, and the GEOS-CHEM model indicate that the 15 April event consisted of trace gases and particles from both Asian anthropogenic and Southeast Asian biomass-burning emissions, while the major sources of the May events were Siberian biomass fires from the early 2002 Russian fire season. To the best of our knowledge, these were the first observations of spring-time transpacific transport of Siberian biomass-burning emissions to the NE Pacific.

[40] We found that the four events had comparable O₃ enhancement ratios ($\Delta\text{O}_3/\Delta\text{CO}$) that ranged from 0.22 to 0.42 mol mol⁻¹. The positive $\Delta\text{O}_3/\Delta\text{CO}$ ratio indicates that all of these events were efficient at transporting O₃ to the NE Pacific troposphere. In contrast, our measurements of aerosol scattering relative to CO ($\Delta\sigma_{\text{sp}(550\text{ nm})}/\Delta\text{CO}$) in the May events are at least twice as great as those observed in the 15 April plume (0.51–0.99 Mm⁻¹ ppbv⁻¹ and 0.27–0.36 Mm⁻¹ ppbv⁻¹, respectively), indicating that the May fires also had significant impacts on particulate levels of the NE Pacific troposphere during the PHOBEA 2002 campaign. The enhancement ratios of ethane, ethyne, and propane (with respect to CO) were similar throughout the four events, with respective means of $(9.9 \pm 0.7) \times 10^{-3}$, $(4.2 \pm 0.5) \times 10^{-3}$, and $(2.7 \pm 0.8) \times 10^{-3}$ mol mol⁻¹ and are consistent with emission ratios from fossil fuel, biofuel, and biomass burning. However, methyl chloride enhancements were very small or negligible during the May events, yet this is consistent with our current knowledge of VOC emissions from temperate and boreal forest fires. Additionally, the methyl chloride enhancements observed during the 15 April event, coupled with the GEOS-CHEM results, indicate that a portion of this plume contained Asian biomass-burning emissions, which possi-

bly include sources such as biofuel and agricultural waste burning.

[41] **Acknowledgments.** The authors would like to thank Peter Weiss-Penzias, Julie Snow, Anna McClintick, and Arrie Symmes for their helpful role in the PHOBEA 2002 airborne campaign. We also wish to acknowledge Jim Grant, Steen Bramer, Jeremy Grogan, and Tom Kelso of Northway Aviation for their flying expertise. We wish to thank the University of Maryland Department of Geography for providing MODIS fire detection data for April and May 2002. We also wish to acknowledge that the GEOS-CHEM model is managed by the Atmospheric Chemistry Modeling Group at Harvard University with support from the NASA Atmospheric Chemistry Modeling and Analysis Program. This research was supported by funds provided by the National Science Foundation grant ATM-0089929 and the National Oceanic and Atmospheric Administration Office of Global Programs NA16GP1586.

References

- Andreae, M. O., and P. Merlet (2001), Emission of trace gases and aerosols from biomass burning, *Global Biogeochem. Cycles*, *15*, 955–966.
- Andreae, M. O., H. Berresheim, T. W. Andreae, M. A. Kritz, T. S. Bates, and J. T. Merrill (1988), Vertical distribution of dimethylsulfide, sulfur dioxide, aerosol ions, and radon over the Northeast Pacific Ocean, *J. Atmos. Chem.*, *6*, 149–173.
- Andreae, M. O., et al. (1996), Methyl halide emissions from savanna fires in southern Africa, *J. Geophys. Res.*, *101*, 23,603–23,613.
- Bernsten, T. K., S. Karlsdottir, and D. A. Jaffe (1999), Influence of Asian emissions on the composition of air reaching the North Western United States, *Geophys. Res. Lett.*, *26*, 2171–2174.
- Bey, I., D. J. Jacob, R. M. Yantosca, J. A. Logan, B. D. Field, A. M. Fiore, Q. Li, H. Y. Liu, L. J. Mickley, and M. G. Schultz (2001a), Global modeling of tropospheric chemistry with assimilated meteorology: Model description and evaluation, *J. Geophys. Res.*, *106*, 23,073–23,096.
- Bey, I., D. J. Jacob, J. A. Logan, and R. M. Yantosca (2001b), Asian chemical outflow to the Pacific: Origins, pathways, and budgets, *J. Geophys. Res.*, *106*, 23,097–23,114.
- Blake, N. J., D. R. Blake, C. Sive, T. Y. Chen, F. S. Rowland, J. E. Collins Jr., G. W. Sachse, and B. E. Anderson (1996), Biomass burning emissions and vertical distribution of atmospheric methyl halides and other reduced carbon gases in the South Atlantic region, *J. Geophys. Res.*, *101*, 24,151–25,164.
- Blake, N. J., et al. (2003), NMHCs and halocarbons in Asian continental outflow during the Transport and Chemical Evolution over the Pacific (TRACE-P) Field Campaign: Comparison with PEM-West B, *J. Geophys. Res.*, *108*(D20), 8806, doi:10.1029/2002JD003367.
- Bognar, J. A., and J. W. Birks (1996), Miniaturized ultraviolet ozonesonde for atmospheric measurements, *Anal. Chem.*, *68*, 3059–3062.
- Cahoon, D. R., Jr., B. J. Stocks, J. S. Levine, W. R. Cofer II, and J. M. Pierson (1994), Satellite analysis of the severe 1987 forest fires in northern China and southeastern Siberia, *J. Geophys. Res.*, *99*, 18,627–18,638.
- Cahoon, D. R., Jr., B. J. Stocks, J. S. Levine, W. R. Cofer III, and J. A. Barber (1996), Monitoring the 1992 forest fires in the boreal ecosystem using NOAA AVHRR satellite imagery, in *Biomass Burning and Global Change*, edited by J. S. Levine, pp. 795–801, MIT Press, Cambridge, Mass.
- Cofer, W. R., III, E. L. Winstead, B. J. Stocks, L. W. Overbay, J. G. Goldammer, D. R. Cahoon, and J. S. Levine (1996), Emissions from boreal forest fires: Are the atmospheric impacts underestimated?, in *Biomass Burning and Global Change*, edited by J. S. Levine, pp. 834–839, MIT Press, Cambridge, Mass.
- Conard, S. G., et al. (2002), Determining effects of area burned and fire severity on carbon cycling and emissions in Siberia, *Clim. Change*, *55*, 197–211.
- Crutzen, P. J., L. E. Heidt, J. P. Krasneck, W. H. Pollock, and W. Seiler (1979), Biomass burning as a source of atmospheric trace gases: CO, H₂, N₂O, NO, CH₃Cl, and COS, *Nature*, *282*, 253–256.
- Doskey, P. V., and H. M. Bialk (2001), Automated sample for the measurement of non-methane organic compounds, *Environ. Sci. Technol.*, *35*, 591–594.
- Duncan, B. N., R. V. Martin, A. C. Staudt, R. Yevich, and J. A. Logan (2003), Interannual and seasonal variability of biomass burning emissions constrained by satellite observations, *J. Geophys. Res.*, *108*(D2), 4100, doi:10.1029/2002JD002378.
- Fiore, A. M., D. J. Jacob, I. Bey, R. M. Yantosca, B. D. Field, A. C. Fusco, and J. G. Wilkinson (2002), Background ozone over the United States in summer: Origin, trend, and contributions to pollution episodes, *J. Geophys. Res.*, *107*(D15), 4275, doi:10.1029/2001JD000982.

- FIRESCAN Science Team (1996), Fire in ecosystems of boreal Eurasia: The Bor forest island fire experiment fire research campaign Asia-North (FIRESCAN), in *Biomass Burning and Global Change*, edited by J. S. Levine, pp. 848–873, MIT Press, Cambridge, Mass.
- Forster, C., et al. (2001), Transport of boreal forest fire emissions from Canada to Europe, *J. Geophys. Res.*, *106*, 22,887–22,906.
- Gerbig, C., D. Kley, A. Volz-Thomas, J. Kent, K. Dewey, and D. S. McKenna (1996), Fast response resonance fluorescence CO measurements aboard the C-130: Instrument characterization and measurements made during North Atlantic Regional Experiment 1993, *J. Geophys. Res.*, *101*, 29,229–29,238.
- Gerbig, C., S. Schmitgen, D. Kley, A. Volz-Thomas, K. Dewey, and D. Haaks (1999), An improved fast-response vacuum-UV resonance fluorescence CO instrument, *J. Geophys. Res.*, *104*, 1699–1704.
- Goode, J. G., R. J. Yokelson, D. E. Ward, R. A. Susott, R. E. Babbitt, M. A. Davies, and W. M. Hao (2000), Measurements of excess O₃, CO₂, CO, CH₄, C₂H₄, C₂H₂, HCN, NO, NH₃, HCOOH, CH₃COOH, HCHO, and CH₃OH in 1997 Alaskan biomass burning plumes by airborne Fourier transform infrared spectroscopy (AFTIR), *J. Geophys. Res.*, *105*, 22,147–22,166.
- Hegg, D. A., L. F. Radke, P. V. Hobbs, R. A. Rasmussen, and P. J. Riggan (1990), Emissions of some trace gases from some biomass fires, *J. Geophys. Res.*, *95*, 5669–5675.
- Hobbs, P. V., P. Sinha, R. J. Yokelson, T. J. Christian, D. R. Blake, S. Gao, T. W. Kirchstetter, T. Novakov, and P. Pilewskie (2003), Evolution of gases and particles from a savanna fire in South Africa, *J. Geophys. Res.*, *108*(D13), 8485, doi:10.1029/2002JD002352.
- Hoell, J. M., D. D. Davis, S. C. Liu, R. E. Newell, H. Akimoto, R. J. McNeal, and R. J. Bendura (1997), The Pacific Exploratory Mission-West: Phase B: February-March, 1994, *J. Geophys. Res.*, *102*, 28,223–28,239.
- Husar, R. B., et al. (2001), Asian dust events of April 1998, *J. Geophys. Res.*, *106*, 18,317–18,330.
- Jacob, D. J., et al. (1992), Summertime photochemistry of the troposphere at high northern latitudes, *J. Geophys. Res.*, *97*, 16,421–16,431.
- Jacob, D. J., J. A. Logan, and P. P. Murti (1999), Effect of rising Asian emissions on surface ozone in the United States, *Geophys. Res. Lett.*, *26*, 2175–2178.
- Jacob, D. J., J. H. Crawford, M. M. Kleb, V. S. Connors, R. J. Bendura, J. L. Raper, G. W. Sachse, J. C. Grille, L. Emmons, and C. L. Heald (2003), The Transport and Chemical Evolution over the Pacific (TRACE-P) aircraft mission: Design, execution, and first results, *J. Geophys. Res.*, *108*(D20), 9000, doi:10.1029/2002JD003276.
- Jaeglé, L., D. Jaffe, H. U. Price, P. Weiss-Penzias, P. I. Palmer, M. J. Evans, D. J. Jacob, and I. Bey (2003), Sources and budgets for CO and O₃ in the northeastern Pacific during the spring of 2001: Results from the PHOBEA-II experiment, *J. Geophys. Res.*, *108*(D20), 8802, doi:10.1029/2002JD003121.
- Jaffe, D. A., T. Anderson, D. Covert, R. Kotchenruther, B. Trost, J. Danielson, W. Simpson, T. Bernsten, S. Karlsdotir, D. Blake, J. Harris, G. Carmichael, and I. Uno (1999), Transport of Asian air pollution to North America, *Geophys. Res. Lett.*, *26*, 711–714.
- Jaffe, D. A., T. Anderson, D. Covert, B. Trost, J. Danielson, W. Simpson, D. Blake, J. Harris, and D. Streets (2001), Observations of ozone and related species in the Northeast Pacific during the PHOBEA Campaigns: 1. Ground-based observations at Cheeka Peak, *J. Geophys. Res.*, *106*, 7449–7461.
- Jaffe, D. A., I. MacKendry, T. Anderson, and H. Price (2003), Six “new” episodes of trans-Pacific transport of air pollutants, *Atmos. Environ.*, *37*, 391–404.
- Justice, C. O., L. Giglio, S. Korontzi, J. Owens, J. T. Morissette, D. Roy, J. Descloitres, S. Alleaume, F. Petitcolin, and Y. Kaufman (2002), The MODIS fire products, *Remote Sens. Environ.*, *83*, 244–262.
- Kasischke, E. S., and L. P. Bruhwiler (2002), Emissions of carbon dioxide, carbon monoxide, and methane from boreal fires in 1998, *J. Geophys. Res.*, *107*, 8146, doi:10.1029/2001JD000461 [printed 108(D1), 2003].
- Kasischke, E. S., K. Bergen, R. Fennimore, F. Sotelo, G. Stephens, A. Janetos, and H. H. Shugart (1999), Satellite imagery gives a clear picture of Russia's boreal forest fires, *Eos Trans. American Geophysical Union*, *80*, 141, 147.
- Kotchenruther, R. A., D. A. Jaffe, H. J. Beine, T. L. Anderson, J. W. Bottenheim, J. M. Harris, D. R. Blake, and R. Schmitt (2001a), Observations of ozone and related species in the northeast Pacific during the PHOBEA campaigns: 2. Airborne Observations, *J. Geophys. Res.*, *106*, 7463–7483.
- Kotchenruther, R. A., D. A. Jaffe, and L. Jaeglé (2001b), Ozone photochemistry and the role of peroxyacetyl nitrate in the springtime northeastern Pacific troposphere: Results from the Photochemical Ozone Budget of the Eastern North Pacific Atmosphere (PHOBEA) campaign, *J. Geophys. Res.*, *106*, 28,731–28,742.
- Kritz, M. A., J. C. LeRouley, and E. F. Danielsen (1990), The China Clipper—Fast advective transport of radon-rich air from the Asian boundary layer to the upper troposphere near California, *Tellus, Ser. B*, *42*, 46–61.
- Lavoue, D., C. Lioussé, H. Cachier, B. J. Stocks, and J. G. Goldammer (2000), Modeling of carbonaceous particles emitted by boreal and temperate wildfires at northern latitudes, *J. Geophys. Res.*, *105*, 26,871–26,890.
- Levine, J. S., and W. R. Cofer III (2000), Boreal forest fire emissions and the chemistry of the atmosphere, in *Fire, Climate, and Carbon Cycling in the Boreal Forest*, edited by E. S. Kasischke and B. J. Stocks, pp. 31–48, Springer-Verlag, New York.
- Li, Q., et al. (2002a), Transatlantic transport of pollution and its effects on surface ozone in Europe and North America, *J. Geophys. Res.*, *107*(D13), 4166, doi:10.1029/2001JD001422.
- Li, Q., D. J. Jacob, T. D. Fairlie, H. Liu, R. M. Yantosca, and R. V. Martin (2002b), Stratospheric versus pollution influences on ozone at Bermuda: Reconciling past analyses, *J. Geophys. Res.*, *107*(D22), 4611, doi:10.1029/2002JD002138.
- Li, Q., D. J. Jacob, R. M. Yantosca, C. L. Heald, H. B. Singh, M. Koike, Y. Zhao, G. W. Sachse, and D. G. Streets (2003), A global three-dimensional model analysis of the atmospheric budgets of HCN and CH₃CN: Constraints from aircraft and ground measurements, *J. Geophys. Res.*, *108*(D21), 8827, doi:10.1029/2002JD003075.
- Liang, Q., L. Jaeglé, D. A. Jaffe, P. Weiss-Penzias, A. Heckman, and J. A. Snow (2004), Long-range transport of Asian pollution to the northeast Pacific: Seasonal variations and transport pathways of carbon monoxide, *J. Geophys. Res.*, *109*, D23S07, doi:10.1029/2003JD004402, in press.
- Liu, H., D. J. Jacob, L. Y. Chan, S. J. Oltmans, I. Bey, R. M. Yantosca, J. M. Harris, B. N. Duncan, and R. V. Martin (2002), Sources of tropospheric ozone along the Asian Pacific Rim: An analysis of ozonesonde observations, *J. Geophys. Res.*, *107*(D21), 4573, doi:10.1029/2001JD002005.
- Liu, H., D. J. Jacob, I. Bey, R. M. Yantosca, B. N. Duncan, and G. W. Sachse (2003), Transport pathways for Asian pollution outflow over the Pacific: Interannual and seasonal variations, *J. Geophys. Res.*, *108*(D20), 8786, doi:10.1029/2002JD003102.
- Lobert, J. M., W. C. Keene, J. A. Logan, and R. Yevich (1999), Global chlorine emissions from biomass burning: Reactive chlorine emissions inventory, *J. Geophys. Res.*, *104*, 8373–8398.
- Martin, R. V., et al. (2002), Interpretation of TOMS observations of tropical tropospheric ozone with a global model and in-situ observations, *J. Geophys. Res.*, *107*(D18), 4351, doi:10.1029/2001JD001480.
- Martin, R. V., D. J. Jacob, R. M. Yantosca, M. Chin, and P. Ginoux (2003), Global and regional decreases in tropospheric oxidants from photochemical effects of aerosols, *J. Geophys. Res.*, *108*(D3), 4097, doi:10.1029/2002JD002622.
- Mauzerall, D. L., D. J. Jacob, S. M. Fan, J. D. Bradshaw, G. L. Gregory, G. W. Sachse, and D. R. Blake (1996), Origin of tropospheric ozone at remote high northern latitudes in summer, *J. Geophys. Res.*, *101*, 4175–4188.
- Mauzerall, D. L., J. A. Logan, D. J. Jacob, B. E. Anderson, D. R. Blake, J. D. Bradshaw, B. Heikes, G. W. Sachse, H. Singh, and B. Talbot (1998), Photochemistry in biomass burning plumes and implications for tropospheric ozone over the tropical South Atlantic, *J. Geophys. Res.*, *103*, 8401–8423.
- McKendry, I. G., J. P. Hacker, R. Stull, S. Sakiyama, D. Mignacca, and K. Reid (2001), Long-range transport of Asian dust to the Lower Fraser Valley, British Columbia, Canada, *J. Geophys. Res.*, *106*, 18,361–18,370.
- Merrill, J. T., R. Bleck, and L. Avila (1985), Modeling atmospheric transport to the Marshall Islands, *J. Geophys. Res.*, *90*, 12,972–12,936.
- Merrill, J. T., M. Uematsu, and R. Bleck (1989), Meteorological analysis of long range transport of mineral aerosol over the North Pacific, *J. Geophys. Res.*, *94*, 8584–8598.
- Newell, R. E., and E. J. Evans (2000), Seasonal changes in pollutant transport to the North Pacific: The relative importance of Asian and European sources, *Geophys. Res. Lett.*, *27*, 2509–2512.
- Palmer, P. I., D. J. Jacob, K. Chance, R. V. Martin, R. J. D. Spurr, T. P. Kurosu, I. Bey, R. Yantosca, A. Fiore, and Q. Li (2001), Air mass factor formulation for spectroscopic measurements from satellites: Application to formaldehyde retrievals from GOME, *J. Geophys. Res.*, *106*, 14,539–14,550.
- Palmer, P. I., D. J. Jacob, D. B. A. Jones, C. L. Heald, R. M. Yantosca, J. A. Logan, G. W. Sachse, and D. G. Streets (2003), Inverting for emissions of carbon monoxide from Asia using aircraft observations over the western Pacific, *J. Geophys. Res.*, *108*(D21), 8828, doi:10.1029/2003JD003397.
- Parrish, D. D., C. J. Hahn, E. J. Williams, R. B. Norton, F. C. Fehsenfeld, H. B. Singh, J. D. Shetter, B. W. Gandrud, and B. A. Ridley (1992), Indication of photochemical histories of Pacific air masses from measure-

- ments of atmospheric trace species at Point Arena, California, *J. Geophys. Res.*, *97*, 15,883–15,901.
- Parrish, D. D., J. S. Holloway, M. Trainer, P. C. Murphy, G. L. Forbes, and F. C. Fehsenfeld (1993), Export of North American ozone pollution to the North Atlantic Ocean, *Science*, *259*, 1436–1439.
- Price, H. U., D. A. Jaffe, P. V. Doskey, I. McKendry, and T. L. Anderson (2003), Vertical profiles of O₃, aerosols, CO and NMHCs in the North-east Pacific during the TRACE-P and ACE-ASIA experiments, *J. Geophys. Res.*, *108*(D20), 8799, doi:10.1029/2002JD002930.
- Price, H. U., D. A. Jaffe, O. R. Cooper, and P. V. Doskey (2004), Photochemistry, ozone production, and dilution during long-range transport episodes from Eurasia to the northwest United States, *J. Geophys. Res.*, *109*, D23S13, doi:10.1029/2003JD004400.
- Radke, L. F., D. A. Hegg, P. V. Hobbs, D. J. Nance, J. H. Lyons, K. Laursen, R. E. Weiss, P. J. Riggan, and D. E. Ward (1991), Particulate and trace gas emissions from large biomass fires in North America, in *Global Biomass Burning: Atmospheric, Climatic, and Biospheric Implications*, edited by J. S. Levine, pp. 209–224, MIT Press, Cambridge, Mass.
- Reid, J. S., and P. V. Hobbs (1998), Physical and optical properties of young smoke from individual biomass fires in Brazil, *J. Geophys. Res.*, *103*, 32,013–32,030.
- Reid, J. S., P. V. Hobbs, R. J. Ferek, D. R. Blake, J. V. Martins, M. R. Dunlap, and C. Liousse (1998), Physical, chemical, and optical properties of regional hazes dominated by smoke in Brazil, *J. Geophys. Res.*, *103*, 32,059–32,080.
- Snow, J. A., J. B. Dennison, D. A. Jaffe, H. U. Price, J. K. Vaughan, and B. Lamb (2003), Aircraft and surface observations in Puget Sound and a comparison to a regional model, *Atmos. Environ.*, *37*, 4019–4032.
- Streets, D. G., and S. T. Waldhoff (1999), Present and future emissions of air pollutants in China: SO₂, NO_x, and CO, *Atmos. Environ.*, *34*, 363–374.
- Stocks, B. J. (1991), The extent and impact of forest fires in northern circumpolar countries, in *Global Biomass Burning: Atmospheric, Climatic, and Biospheric Implications*, edited by J. S. Levine, pp. 197–202, MIT Press, Cambridge, Mass.
- Sukhinin, A. I., V. V. Ivanov, E. I. Ponomarev, O. A. Slinkina, A. V. Cherepanov, E. A. Pavlichenko, V. Y. Romansko, and S. I. Miskiv (2003), The 2002 fire season in the Asian part of the Russian Federation, *Int. Forest Fire News*, *28*, 17–27.
- Susott, R. A., D. E. Ward, R. E. Babbitt, and D. J. Latham (1991), Measurement of trace gas emissions and combustion characteristics for a mass fire, in *Global Biomass Burning: Atmospheric, Climatic, and Biospheric Implications*, edited by J. S. Levine, pp. 245–257, MIT Press, Cambridge, Mass.
- Ward, D. E., and C. C. Hardy (1991), Smoke emissions from wildland fires, *Environ. Int.*, *17*, 117–134.
- Weiss-Penzias, P., D. A. Jaffe, L. Jaeglé, and Q. Liang (2004), Influence of long-range-transported pollution on the annual and diurnal cycles of carbon monoxide and ozone at Cheeka Peak Observatory, *J. Geophys. Res.*, *109*, D23S14, doi:10.1029/2004JD004505, in press.
- Wofsy, S. C., et al. (1992), Atmospheric chemistry in the Arctic and Subarctic: Influence of natural fires, industrial emissions, and stratospheric inputs, *J. Geophys. Res.*, *97*, 16,731–16,746.
- Wotawa, G., and M. Trainer (2000), The influence of Canadian forest fires on pollutant concentrations in the United States, *Science*, *288*, 324–328.
- Yokelson, R. J., D. E. Ward, R. A. Susott, J. Reardon, and D. W. T. Griffith (1997), Emissions from smoldering combustion of biomass measured by open-path Fourier transform infrared spectroscopy, *J. Geophys. Res.*, *102*, 18,865–18,877.
- Yokelson, R. J., I. T. Bertschi, T. J. Christian, P. V. Hobbs, D. E. Ward, and W. M. Hao (2003), Trace gas measurements in nascent, aged, and cloud-processed smoke from African savanna fires by airborne Fourier transform infrared (AFTIR) spectroscopy, *J. Geophys. Res.*, *108*(D13), 8478, doi:10.1029/2002JD002322.

I. T. Bertschi, J. B. Dennison, and D. A. Jaffe, Department of Interdisciplinary Arts and Sciences, University of Washington-Bothell, 18115 Campus Way NE, Bothell, WA 98011, USA. (isaacpb@u.washington.edu; dennison@u.washington.edu; djaffe@u.washington.edu)

L. Jaeglé and H. U. Price, Department of Atmospheric Sciences, University of Washington, Box 351640, Seattle, WA 98195, USA. (jaegle@atmos.washington.edu; hprice@u.washington.edu)

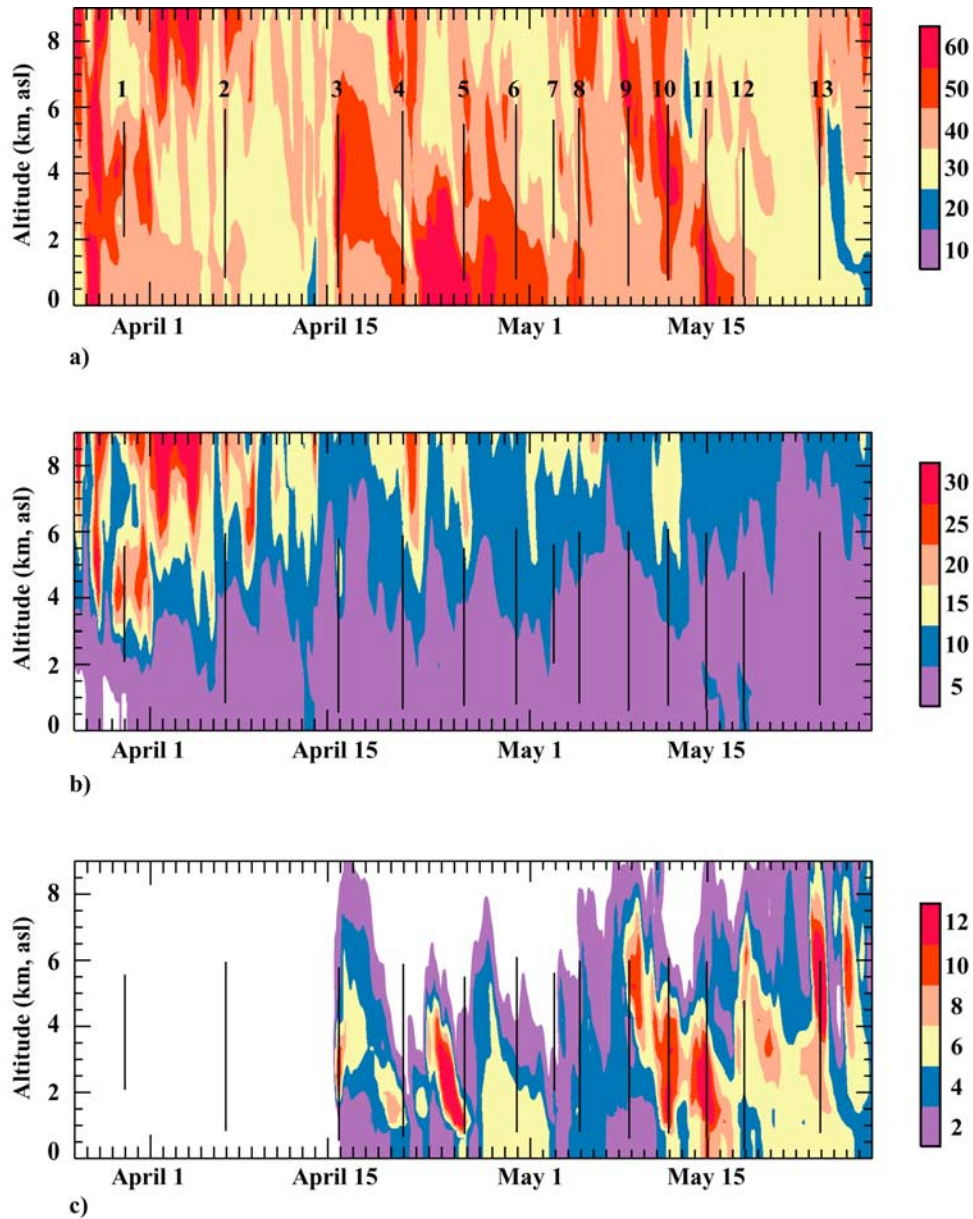


Figure 6. GEOS-CHEM time-height cross sections of the tagged-CO simulation at CPO (48.3°N , 124.6°W) throughout the spring of 2002. The numbered vertical lines show the vertical range of the PHOBEA 2002 research flights. The cross sections show (a) Asian anthropogenic, (b) Southeast Asian biomass burning, and (c) Siberian biomass burning sources of CO. Note that each CO cross section is scaled differently.